Use of vanadocene as an organometallic reducing agent for the preparation of ultrafine magnetic iron powder and organized iron particles from iron salts‡

Robert Choukroun,*[a] Dominique de Caro,[a] Sandrine Matéo,[a] Catherine Amiens,[a] Bruno Chaudret,*[a] Etienne Snoeck[b] and Marc Respaud[c]

[a] *Laboratoire de Chimie de Coordination du CNRS (CNRS UPR 8241)†, 205, route de Narbonne, 31077 Toulouse cedex, France*
[b] *CEMES-LOE-CNRS, 29, rue Jeanne Marvig, BP 4347, 31055 Toulouse cedex, France*
[c] *Laboratoire de Physique de la Matière Condensée — Service National des Champs Magnétiques Pulsés, INSA, Complexe Scientifique de Rangueil, 31077 Toulouse cedex, France*

A THF suspension of $FeCl_2$ reacts with the 15-electron complex, vanadocene $[V(C_5H_5)_2]$ to give ultrafine magnetic Fe powder. X-Ray diffraction and Mössbauer spectra confirm the presence of the α-iron phase. The average crystallite size was estimated to be 18 nm and the magnetic hyperfine field was found to be 341 kG at 100 K, as expected for fine iron particles. A typical ferromagnetic behaviour was observed for the powder in the 5–300 K range. Saturation magnetization at 5 K (223 emu g_{Fe}^{-1}), very close to the value for bulk α-Fe, revealed the presence of small α-iron particles without iron oxide contaminant at the surface. The same reaction carried out in the presence of polyvinylpyrrolidone (PVP) yields PVP-protected zerovalent iron particles. Mössbauer analysis revealed the presence of 83% Fe^0 and 17% unreduced $FeCl_2$. The sample exhibits ferromagnetic behaviour with saturation magnetization (*ca.* 240 emu g_{Fe}^{-1}) comparable to the bulk value, confirming the presence of small zerovalent nanoparticles. HREM experiments performed at high magnification display small Fe particles (diameter of about 8 nm) agglomerated into 50–200 nm superstructures. The particles show an astonishing common magnetic and crystallographic orientation.

Research towards the preparation and properties of ultrafine metal powders and metal colloids spans many areas of interest such as catalysis,[1,2] magnetic materials[3–5] and materials for optics.[6] In 1975, Rieke reported a general approach for preparing highly reactive metal powders by reducing metal salts in diethyl ether or hydrocarbon solvents using alkali metals (Na or K).[7] An alternative method is the preparation of finely divided, highly reactive metal powders from metal salts using magnesium–anthracene systems as reducing agents.[8,9] This method, developed by Bogdanovic and co-workers, was used to prepare powders of elements of Groups 8–12. The reduction of a metal halide by metallic magnesium in organic solution was also described and led to finely divided ferromagnetic metals and alloys.[10] Alternative methods for the preparation of fine metal powders involve metal evaporation,[3,4] sonolysis of volatile carbonyl complexes,[11] high temperature reduction of monodispersed metal oxides[12,13] and chemical reduction of metal salts by alkali or alkaline earth metal hydridotriorganoborates or gallates.[14] This latter process, developed by Bönnemann and co-workers, led to the preparation of boride-free metal nanopowders including elements of Groups 6–12 and 14. Finally, Dye and co-workers prepared nanoscale metal powders through the reduction of metal salts by a solution containing solvated electrons (e_s^-) or alkali metal anions.[15]

Several methods have recently been reported for the synthesis of colloids of ferromagnetic metals (Fe, Co, Ni). This includes sonication of $Fe(CO)_5$ in the presence of a protecting polymer,[16,17] decomposition of organometallic precursors,[18,19] reduction in reverse micelles[20,21] and electrochemical generation in the presence of surfactants.[22]

We describe in this paper a new and simple method for the preparation of ultrafine iron powder and iron colloids in a polymer matrix, using 15-electron vanadocene as an organometallic reducing agent in organic solution, as well as their characterization by physical techniques including HREM (high resolution electron microscopy).

Results and Discussion

The reducing properties of V^{II} in the chemistry of metal colloids have previously been studied.[23] V_{aq}^{2+} ions were obtained by reduction of $VOSO_4$ solution over amalgamated zinc. Addition of V_{aq}^{2+} into solutions of copper(II) salts containing organic polymers as stabilizers led to copper colloids whose average particle size varies over a wide range (2–500 nm), depending on the nature and the concentration of all the reagents. However, to the best of our knowledge, we describe for the first time the use of a well-characterized organometallic V^{II} complex, namely $V(C_5H_5)_2$, for preparing nanostructured powders and colloids.

In a preliminary experiment, we showed that the reaction of $FeCl_2$ with $V(C_5H_5)_2$ (2 molar equiv.) in tetrahydrofuran (THF) and in the presence of CO led to $Fe(CO)_5$ as revealed by infrared spectroscopy.[24] This demonstrated the capability of vanadocene to reduce Fe^{II} into highly reactive Fe^0 atoms.

Ultrafine iron powder

The reduction of $FeCl_2$ with 2 equiv. of $V(C_5H_5)_2$ in THF at room temperature leads to ultrafine iron powder. A change in the colour of the solution from purple to blue indicates the

* Fax: +33 5 61 55 30 03; e-mail: choukrou@lcc-toulouse.fr, chaudret@lcc-toulouse.fr
† Liée par convention à l'Université Paul Sabatier et à l'Institut National Polytechnique de Toulouse.
‡ Non-SI units employed: 1 emu = 10^{-3} A m^2; 1 G = 10^{-4} T; 1 Ci = 3.7×10^{10} Bq.

oxidation of $V(C_5H_5)_2$ into $V(C_5H_5)_2Cl$. Electrochemical studies in THF reveal that the oxidation of $V(C_5H_5)_2$ involves two one-electron transfer reactions, the first (*ca.* −0.7 V *vs.* SCE) reversible and the second irreversible, possibly due to the formation of a solvated species $[V(C_5H_5)_2(THF)_2]^{2+}$ (the position of this latter peak is highly dependent on the scan rate).[25] $FeCl_2$ is not THF soluble and its redox potential cannot be measured in this solvent. It is consequently not possible to compare it with the value corresponding to $V(C_5H_5)_2^{+}/V(C_5H_5)_2$ (−0.7 V *vs.* SCE in THF). However, the redox potential corresponding to Fe^{2+}/Fe is *ca.* −0.5 V *vs.* SCE in water at pH = 0. THF being a less good electron donor than water, the reduction of Fe^{II} into Fe^0 is then conceivable. Iron powder can be easily purified by washing several times with THF to eliminate $V(C_5H_5)_2Cl$ and possibly unreacted $V(C_5H_5)_2$.

The X-ray diffraction (XRD) spectrum displays the characteristic lines of α-iron metal at θ = 22.4°, 32.6° and 41.2° (*d* spacings of 2.02, 1.43 and 1.17 Å, respectively) as shown on Fig. 1. Three other small lines at 21.6°, 23.8° and 24.3° were also observed; these were not attributed but they do not correspond to iron oxide species. The diffraction peak at Bragg angle θ = 22.4° allowed us, using the Scherrer equation, to estimate the average crystallite size to be 18 nm (±3 nm).[26] Differential thermal analysis (DTA) (carrier gas: Ar) is in agreement with the presence of iron in a nanocrystalline form. The DTA shows no significant peak in the 20–1000 °C range. For amorphous Fe powder, Suslick and co-workers have observed one large exothermic signal, at 308 °C using differential scanning calorimetry, that they attributed to a disorder-order transition (crystallization from amorphous Fe to α-Fe).[11]

The Mössbauer spectrum of Fe powder recorded at 100 K exhibits a hyperfine sextet (isomer shift $\delta = -0.05$ mm s^{-1}) assigned to α-Fe (see Fig. 2). The magnetic hyperfine field H_{eff} has been determined to be 341 kG (cgs, Gaussian). This value is slightly higher than that for bulk α-Fe (337 kG at 82 K) as expected for fine iron particles.[27] Klabunde and co-workers have measured a magnetic hyperfine field of 344 kG (at 77 K) for Fe powder containing α-Fe nanocrystallites with an average size of 7.5 nm as estimated by the BET technique.[3]

Fig. 3 illustrates the variation of the magnetization (*M*) of the powder as a function of applied field (*H*) at 5 K. We note that the saturation magnetization (M_S = 223 emu g_{Fe}^{-1} at 5 K) is very close to the value for bulk α-Fe (217 emu g_{Fe}^{-1} at 0 K),[28] in agreement with the presence of nanocrystalline Fe^0. For oxide-coated α-Fe nanoparticles, much lower saturation magnetizations are observed (⩽150 emu g_{Fe}^{-1}).[29] The saturation magnetization values decrease when the temperature increases, as is generally observed.[30] These values plotted versus $T^{\frac{3}{2}}$ follow Bloch's law.[31] Bloch constant (*B*) was estimated to be 1.5×10^{-5} $K^{-\frac{3}{2}}$, higher than the bulk value of 3.5×10^{-6} $K^{-\frac{3}{2}}$.[32] Thermal fluctuations of the surface moments are larger than those of the inner moments so that *B* of the surface atoms is about 2–3.5 times larger than *B* of the inner atoms. This explains the larger values of *B* in smaller particles, which possess a much higher fraction of surface atoms.[29] At 5 K, there is a small coercive field of $H_c \approx 170$ G. This value is similar to that reported by Suslick and co-workers for amorphous iron powder (*ca.* 190 G at 5 K for grains ⩽30 nm),[28] which suggests that for iron nanoparticles of similar size, the values of the coercive fields at 5 K are comparable in the presence or absence of crystallographic order. Up to 300 K, a ferromagnetic behaviour is observed with a roughly constant coercive field. The iron nanopowder is pyrophoric, which prevented its full characterization by microscopy techniques (TEM or SEM). However, after overnight exposure of a THF suspension to air, the Mössbauer spectrum of the powder collected at 100 K could be fitted to a sextet (isomer shift $\delta = -0.06$ mm s^{-1}, hyperfine field H_{eff} = 339 kG) corresponding to α-Fe (6%) and to a sextet ($\delta = 0.28$ mm s^{-1}, H_{eff} = 522 kG) that has been attributed to α-Fe_2O_3 (94%). This demonstrates the nearly complete oxidation of nanocrystalline Fe into α-Fe_2O_3. A scanning electron micrograph (SEM) of the oxidized powder shows rough pieces of agglomerated particles. Such a SEM profile is often observed for ultrafine crystalline metal and metal-oxide powders,[33,34] whereas amorphous materials show typical conchoidal fractures.[11]

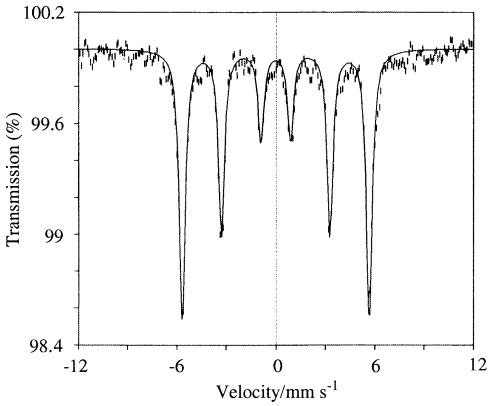

Fig. 2 Mössbauer spectrum of Fe powder collected at 100 K

PVP-protected iron particles

The reaction of a THF suspension of $FeCl_2$ with 2.3 equiv. of $V(C_5H_5)_2$ at room temperature, in the presence of polyvinylpyrrolidone (PVP) as a protecting polymer, leads to the precipitation of iron colloids dispersed in PVP and isolated as

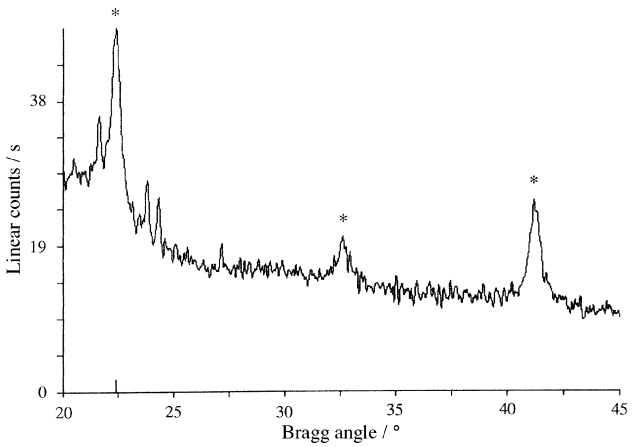

Fig. 1 XRD spectrum of Fe powder (* corresponds to α-Fe)

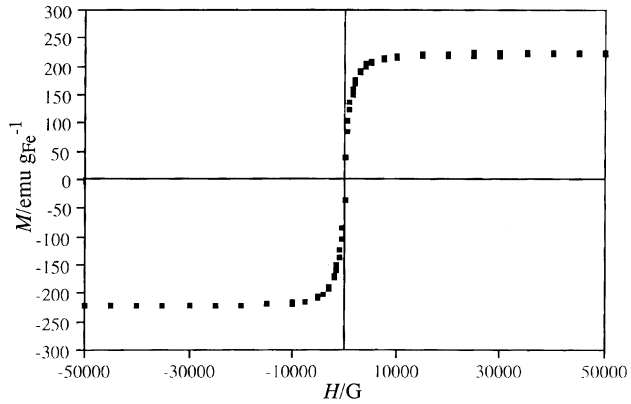

Fig. 3 Magnetization *versus* applied magnetic field for Fe powder (at 5 K)

a dark-grey solid. The Mössbauer spectrum of the solid collected at 100 K could be fitted to a sextet ($\delta = -0.06$ mm s^{-1}, $H_{eff} = 341$ kG) corresponding to Fe^0 (83%) and to a doublet attributed to unreduced $FeCl_2$ (17%) (see Fig. 4). A change in the experimental conditions (initial Fe:PVP weight ratio, reduction time) did not allow us to increase the Fe^0 content.

The size distribution of the nanoparticles was measured from low magnification micrographs (see Fig. 5), which show the presence of agglomerated grains displaying a diameter varying in the range of 50–200 nm. The smaller grains have a spherical shape while the bigger ones exhibit a cubic shape. Selected area electron diffraction (SAED) experiments performed on this powder gave ring patterns typical of bcc Fe particles (inset Fig. 5). On some occasions, rings corresponding to $FeCl_2$ have also been observed. HREM experiments performed at higher magnification demonstrate that each grain consists of an assembly of individual Fe nanoparticles of about 8 nm diameter (Fig. 6). In this image one can also observe a small 40 nm diameter single crystal consisting of residual $FeCl_2$, which has not been reduced. Fig. 7(*a*) shows a microdiffraction pattern obtained on the Fe grain of Fig. 7(*b*). This microdiffraction experiment indicates that the small Fe particles inside this larger grain have a common orientation. Such an observation can also be verified by selecting the 110 reflection and doing a 110 dark field image of the same grain. This dark field image is reported in Fig. 7(*c*) and clearly confirms that inside one large Fe grain, the smaller Fe nanoparticles exhibit a common orientation. This was also observed while studying HREM micrographs obtained on large single grains. The grain formation and common crystallographic orientation may result from the self-assembly of the Fe nanoparticles, which may be induced by a dipolar coupling

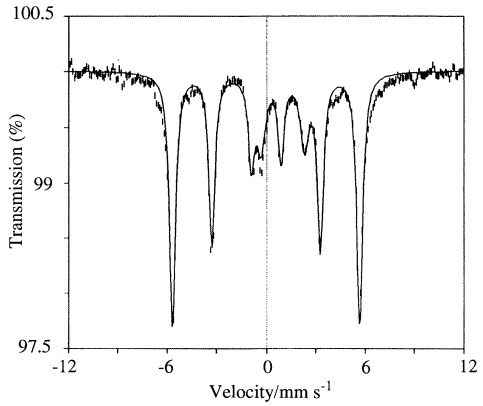

Fig. 4 Mössbauer spectrum of Fe–PVP colloids collected at 100 K

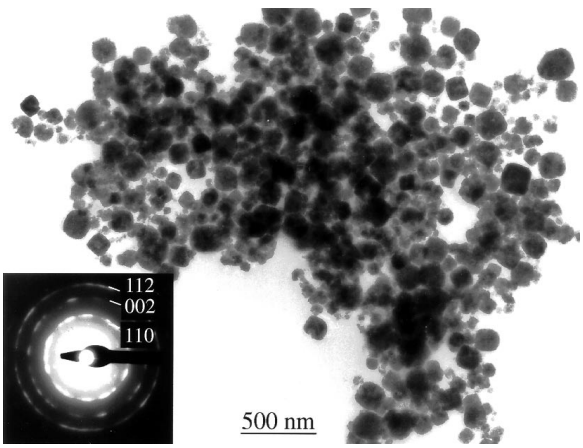

Fig. 5 Low magnification TEM micrograph showing the dispersion and the size of the grains in the Fe–PVP powder with its SAED ring pattern inset

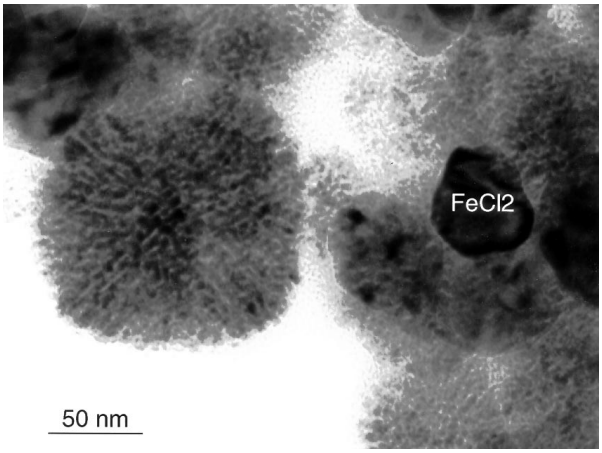

Fig. 6 Higher magnification TEM micrograph showing that the large Fe grains consist in the agglomeration of smaller Fe nanoparticles. The selected area was chosen in order to evidence the presence of some unreduced $FeCl_2$

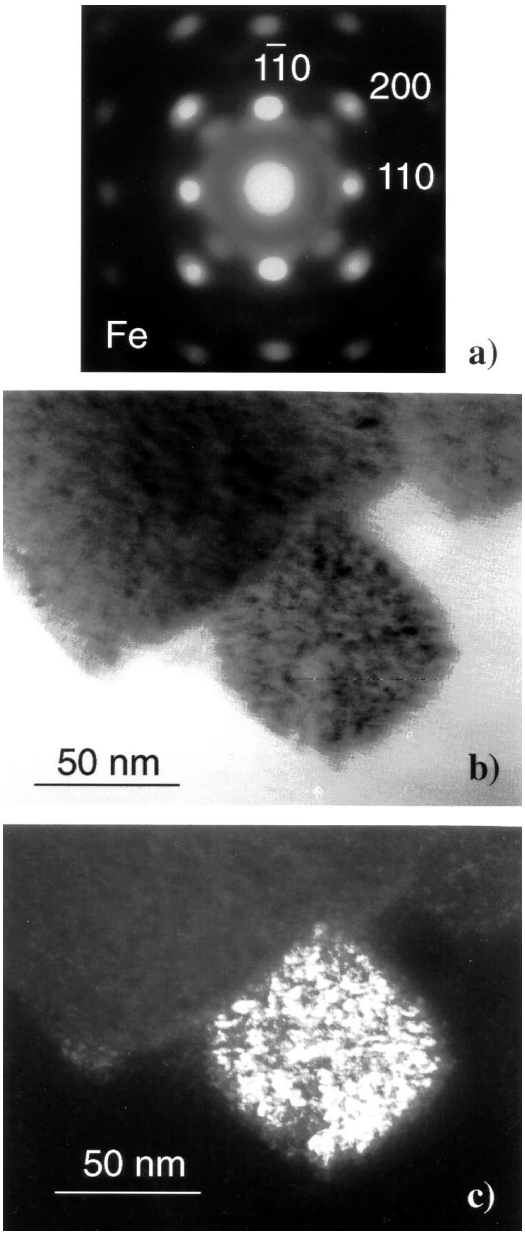

Fig. 7 (*a*) Microdiffraction pattern obtained on the Fe grain shown in (*b*). (*b*) Bright field image of a Fe grain. (*c*) Associated 110 dark field image of the Fe grain

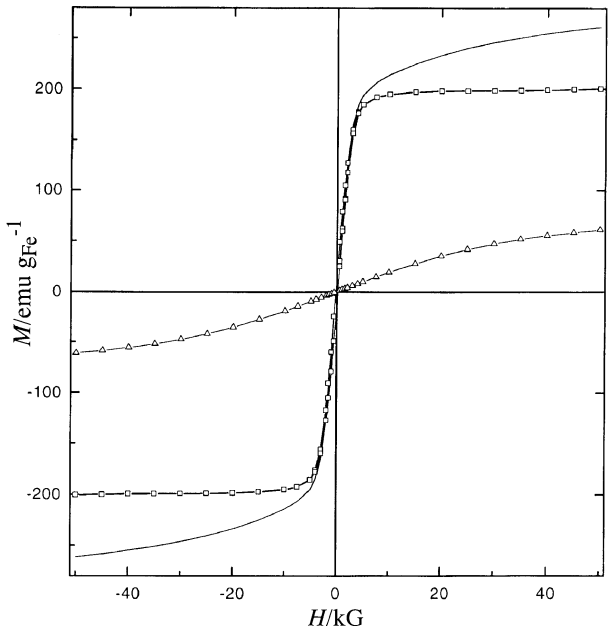

Fig. 8 Magnetization of Fe–PVP solid (solid line) and of Fe^0 nanoparticles (squares) after subtracting the paramagnetic contribution (triangles) measured at 5 K. All magnetizations are normalized *versus* iron mass

between them favouring a parallel orientation of their magnetization. Alternatively, this common orientation may be due to a pseudomorphic reaction. In that case reduction of iron by vanadocene would occur within the channels of the $FeCl_2$ structure and would lead to the precipitation of small Fe^0 grains, all showing the same orientation. Both mechanisms seem possible at the present time, it is, however, remarkable that this method leads to organized superstructures. Such a common orientation is similar to that observed by Matijevic and co-workers in the case of hematite (α-Fe_2O_3) particles obtained by forced hydrolysis of ferric chloride solutions.[35,36] They have demonstrated the presence of typical chain-like ordered structures.

Fig. 8 presents the magnetization curve of the solid measured at 5 K, which does not saturate in fields up to 50 kG. The absence of saturation is due to the presence of paramagnetic impurities. Indeed, chemical microanalysis of the powder reveals the presence of vanadium (probably V^{III}, 0.5 wt%), while the Mössbauer spectrum evidences the presence of Fe^{II}. By subtracting these two paramagnetic contributions from the experimental curve, it is possible to obtain the magnetization due to the particles only. The particles display a ferromagnetic behaviour with a small coercive field of $H_c = 180$ G at 5 K and a saturation magnetization slightly enhanced compared to the bulk value. This confirms the presence of essentially nanocrystalline Fe^0, as observed in Mössbauer and HREM experiments, contaminated with some paramagnetic impurities diluted in the polymer. As observed for the Fe powder, a ferromagnetic behaviour persists for PVP-coated Fe particles, even for temperatures up to 300 K. In the case of individual 8 nm diameter nanoparticles, a classical superparamagnetic behaviour is expected.[37] In our case, big agglomerates with diameters ranging from 50 to 200 nm are present in which strong dipolar couplings[38] between the nanoparticles enhance considerably the blocking temperature, which can be above 300 K.

Conclusions

We report in this paper the facile synthesis of Fe powder and the preparation of sterically protected iron colloids under mild conditions using the highly reactive 15-electron vanadocene complex as a reducing agent.

The crystallographic ordering of nanoparticles is an important challenge for studying the cooperative physical properties of nanoparticles (magnetoresistance for example). The successful synthesis of such a material in the present case is no doubt related to the mild conditions of the synthesis involving organometallic reagents. It is not possible at the present time to determine whether this organization of the nanoparticles results from a self-organization process, the driving force of which is the magnetic dipolar couplings between the particles, or from a pseudomorphic reaction that retains the outside shape of the starting microcrystals of $FeCl_2$ but allows the reduction of Fe and the growth of nanoparticles. Further work is in progress to determine this important point.

This reductive method using vanadocene is complementary to the one involving the decomposition of organometallics by a reducing gas that we have previously used and will be further developed, especially for systems difficult to prepare by other methods. The drawback of the method is presently the presence of small quantities of vanadium in the final material. Future work will be devoted to preparing new materials by this method that avoid the presence of contaminants.

Experimental

All reactions were carried out under an inert Ar atmosphere in a glovebox. THF was purified just before use by distillation over sodium–benzophenone under an argon atmosphere. Anhydrous $FeCl_2$ was purchased from Strem and polyvinylpyrrolidone (PVP) K 30 (average molecular weight 40 000) from Aldrich.

Infrared spectra were recorded in solution on a Perkin–Elmer 1725 FT–IR spectrophotometer. The reference spectrum of THF was subtracted.

The thermal behaviour of Fe powder was studied using a Setaram, model TG-TDA 92, thermoanalyzer allowing simultaneous measurements of TGA (thermal gravimetric analysis) and DTA signals from room temperature up to 1000 °C.

X-Ray diffraction spectra were recorded on a Seifert diffractometer, model XRD 3000 TT, working with Cu-Kα radiation (1.5406 Å).

Mössbauer spectra were collected on a spectrometer operating in the constant acceleration mode with a 50 mCi ^{57}Co source driven by a constant acceleration transducer (Wissel model MA 260). A proportional counter detector with $Kr–CO_2$ fill gas (model LND/Canberra) was used to detect the γ-rays emitted from the sample. The experimental spectra were fitted to a Lorentzian lineshape by a linear least square fitting program. The magnetization studies were carried out using a SQUID magnetometer (MPMS Quantum Design). The temperature has been varied from 5 to 300 K and magnetic fields up to 50 kG were applied. Samples for Mössbauer and SQUID analyses were weighed out in an inert N_2 atmosphere glovebox.

Scanning electron micrographs were obtained using a scanning electron microscope from JEOL, model JSM 840 A.

The size distribution, the morphology and the crystalline structure of the PVP-protected Fe particles were studied by HREM performed on a Philips CM30/ST operating at 300 kV whose point resolution is 0.19 nm. The powder was dissolved in methanol and the resulting solution was poured onto a copper grid covered by a thin carbon film.

Elemental analyses of iron and vanadium were performed by the Service d'Analyses Elémentaires du CNRS à Vernaison.

Syntheses

Synthesis of α-iron powder. A Schlenk tube was charged with 380 mg $FeCl_2$ (3 mmol), 1.08 g $V(C_5H_5)_2$ (6 mmol) and 25 mL THF. The resulting suspension was stirred magnetically for 24 h, then transferred into a glass filter frit. The fine

black Fe powder was washed several times with THF, pentane and finally dried under vacuum (100 mg, 60%). *CAUTION! Fe powder is flammable in air.*

Synthesis of PVP-protected iron colloids. A solution of $V(C_5H_5)_2$ (320 mg, 1.8 mmol) and PVP (70 mg) in 10 mL THF was transferred into a suspension of $FeCl_2$ (100 mg, 0.8 mmol, $[V/Fe]_{molar} = 2.3$) in 10 mL THF. The resulting suspension was stirred for 15 min, during which time the colour changed from purple to blue, indicating the oxidation of $V(C_5H_5)_2$ into $V(C_5H_5)_2Cl$. A supplementary amount of PVP (350 mg in 10 mL THF) was then added. The solution was stirred magnetically for 24 h. PVP-stabilized iron colloids precipitated from the solution and were isolated by filtration. The dark-grey solid thus obtained was washed several times with THF and finally dried (350 mg). The solid is very soluble in alcoholic solvents (elemental analysis: Fe = 10.5 wt%, V = 0.5 wt%).

Acknowledgements

We thank M. Reversat for scanning electron micrographs (ENSCT), J. F. Meunier for Mössbauer experiments (LCC), V. Collière for DTA experiments (LCC), Dr F. Senocq for XRD spectra (ENSCT), A. Mari for magnetic measurements (LCC) and CNRS for support.

References and Notes

1 J. S. Bradley, in *Clusters and Colloids, from Theory to Applications*, ed. G. Schmid, VCH, Weinheim, 1994, pp. 459–544.
2 *Active Metals: Preparation, Characterization, Applications*, ed. A. Fürstner, VCH, Weinheim, 1996.
3 K. A. Easom, K. J. Klabunde, C. M. Sorensen and G. C. Hadjipanayis, *Polyhedron*, 1994, **13**, 1197; S. Brunaeur, P. H. Emmet and E. Teller, *J. Am. Chem. Soc.*, 1938, **60**, 309.
4 K. J. Klabunde and G. Cardenas-Trivino, in ref. 2, pp. 237–277.
5 *Magnetic Properties of Fine Particles*, ed. J.-L. Dormann and D. Fiorani, North-Holland, Amsterdam, 1992.
6 U. Kreibig and M. Vollmer, *Optical Properties of Metal Clusters*, Springer-Verlag, Berlin, 1995.
7 R. D. Rieke, *Top. Curr. Chem.*, 1975, **59**, 1.
8 B. Bogdanovic, *Acc. Chem. Res.*, 1988, **21**, 261.
9 L. E. Aleandri and B. Bogdanovic, in ref. 2, pp. 299–338.
10 J.-M. Broto, J.-C. Ousset, H. Rakoto, S. Askenazy, Ch. Dufor, M. Brieu and P. Mauret, *Solid State Commun.*, 1993, **85**, 263.
11 K. S. Suslick, S. Choe, A. A. Cichowlas and M. W. Grinstaff, *Nature (London)*, 1991, **353**, 414.
12 S. Hamada, M. Eto and Y. Kudo, *J. Chem. Soc. Jpn., Chem. Ind. Chem.*, 1984, **6**, 843.
13 T. Ishikawa and E. Matijevic, *Langmuir*, 1988, **4**, 26.
14 H. Bönnemann and W. Brijoux, in ref. 2, pp. 339–379.
15 K.-L. Tsai and J. Dye, *J. Am. Chem. Soc.*, 1991, **113**, 1650.
16 K. S. Suslick, M. Fang and T. Hyeon, *J. Am. Chem. Soc.*, 1996, **118**, 11960.
17 D. de Caro, T. Ould Ely, A. Mari, B. Chaudret, E. Snoeck, M. Respaud, J.-M. Broto and A. Fert, *Chem. Mater.*, 1996, **8**, 1987.
18 J. Osuna, D. de Caro, C. Amiens, B. Chaudret, E. Snoeck, M. Respaud, J.-M. Broto and A. Fert, *J. Phys. Chem.*, 1996, **100**, 14571.
19 D. de Caro and J. S. Bradley, *Langmuir*, 1997, **12**, 3067.
20 J. P. Wilcoxon, R. L. Williamson and R. J. Baughman, *J. Chem. Phys.*, 1993, **98**, 9933.
21 N. Duxin, O. Stephan, C. Petit, P. Bonville, C. Colliex and M. P. Pileni, *Chem. Mater.*, 1997, **9**, 2096.
22 J. A. Becker, R. Schäfer, R. Festag, W. Ruland, J. H. Wendorff, J. Pebler, S. A. Quaiser, W. Helbig and M. T. Reetz, *J. Chem. Phys.*, 1995, **103**, 2520.
23 E. R. Savinova, A. L. Chuvilin and V. N. Parmon, *J. Mol. Catal.*, 1988, **48**, 217.
24 Two strong CO absorptions at 1994 and 2019 cm^{-1} were seen (solution in THF), similar to those observed for pure liquid $Fe(CO)_5$.
25 J. D. L. Holloway, W. L. Bowden and W. E. Geiger, Jr., *J. Am. Chem. Soc.*, 1977, **99**, 7089.
26 The most widely used equation to calculate the size of nanocrystals is the Scherrer formula: $L = (0.9\ \lambda/\Delta \cos \theta)$ where L = size of nanocrystals (nm), λ = wavelength of the source X-ray (nm), θ = the Bragg angle and Δ = the half-width at half maximum of the diffraction peak (rad).
27 R. S. Preston, S. S. Hanna and J. Heberle, *Phys. Rev.*, 1962, **128**, 2207.
28 M. W. Grinstaff, M. B. Salamon and K. S. Suslick, *Phys. Rev. B*, 1993, **48**, 269.
29 S. Gangopadhyay, G. C. Hajipanayis, B. Dale, C. M. Sorensen, K. J. Klabunde, V. Papaefthymiou and A. Kostikas, *Phys. Rev. B*, 1992, **45**, 9778.
30 C. F. Kernizan, K. J. Klabunde, C. M. Sorensen and G. C. Hadjipanayis, *Chem. Mater.*, 1990, **2**, 70.
31 Saturation magnetization follows Bloch's relation: $M_S(T) = M_S(0)[1 - BT^{\frac{3}{2}}]$ where $M_S(0)$ is the magnetization at 0 K and B is the Bloch constant, see: F. Bloch, *Z. Phys.*, 1931, **61**, 206.
32 C. Kittel, *Introduction to Solid State Physics*, John Wiley, New York, 1971.
33 K. J. Klabunde, H. F. Efner, T. O. Murdock and R. Ropple, *J. Am. Chem. Soc.*, 1976, **98**, 1021.
34 D. Zeng and M. J. Hampden-Smith, *Chem. Mater.*, 1993, **5**, 681.
35 M. Ozaki, H. Suzuki, K. Takahashi and E. Matijevic, *J. Colloid Interface Sci.*, 1986, **113**, 76.
36 M. Ozaki, T. Egami, N. Sugiyama and E. Matijevic, *J. Colloid Interface Sci.*, 1988, **126**, 212.
37 J. L. Dormann, *Rev. Phys. Appl.*, 1981, **16**, 275.
38 S. Morup and H. Topsoe, *J. Magn. Magn. Mater.*, 1983, **31–34**, 953.

Received in Montpellier, France, 4th February 1998;
Paper 8/01094C